

# Rotational evolution of young pulsars due to superfluid decoupling

Wynn C. G. Ho & Nils Andersson \*

\* School of Mathematics, University of Southampton, Southampton, SO17 1BJ, United Kingdom.

---

**Pulsars are rotating neutron stars that are seen to slow down, and the spin-down rate is thought to be due to magnetic dipole radiation.<sup>1,2</sup> This leads to a prediction for the braking index  $n$ , which is a combination of spin period and its first and second time derivatives. However, all observed values<sup>3</sup> of  $n$  are below the predicted value of 3. Here we provide a simple model that can explain the rotational evolution of young pulsars, including the  $n = 2.51$  of the 958-year-old pulsar in the Crab nebula.<sup>4</sup> The model is based on a decrease in effective moment of inertia due to an increase in the fraction of the stellar core that becomes superfluid as the star cools via neutrino emission. The results suggest that future large radio monitoring campaigns of pulsars will yield measurements of the neutron star mass, nuclear equation of state, and superfluid properties.**

---

The core of a neutron star has densities near and above nuclear saturation and extends to ninety percent of the radius of the star; the remaining kilometer or so is the stellar crust. The core is composed of degenerate matter, mostly neutrons and a small fraction of protons and electrons (and possibly exotica, such as hyperons and deconfined quarks, which we do not consider here). Immediately after neutron star formation, this matter is in a normal state due to the high temperatures reached in stellar core collapse. However, neutron stars cool rapidly through the emission of neutrinos, and when the temperature drops below the (density-dependent) critical temperature for Cooper pairing, neutrons and protons form a superfluid and superconductor, respectively.<sup>5,6</sup> Superfluid neutrons rotate by forming quantized vortices, and the spatial distribution of these vortices determines the rotation rate of the superfluid core, e.g., vortices migrate away from the stellar axis of rotation when the superfluid angular velocity  $\Omega_{\text{sf}}$  decreases while  $\Omega_{\text{sf}}$  cannot change if the vortices are fixed in location, i.e., when they are pinned. Meanwhile, normal matter (e.g., in the crust) rotates at an angular velocity  $\Omega$  that decreases as a result of energy loss from the stellar surface due to magnetic dipole radiation, i.e.,  $dE/dt = -\beta\Omega^4$ , where  $\beta \approx B^2 R^6 / 6c^3$  and  $B$  and  $R$  are the neutron star magnetic field and radius, respectively.<sup>1,2</sup>

A rapid decline in surface temperature was recently detected in the 330-year-old neutron star in the Cassiopeia A supernova remnant.<sup>7,8</sup> The observed cooling can be understood as being caused by the recent onset of neutron superfluidity in the core of the star, combined with a much earlier onset of proton superconductivity.<sup>9,8</sup> This has provided the first direct constraints on core superfluid and superconducting properties from neutron star observations.

These new results motivate studies of possible implications. Here we explore the rotational evolution of young pulsars using the newly-constrained superfluid properties and assuming this superfluid core is allowed to decouple (as discussed below). We use simulations<sup>10</sup> of the cooling of a neutron star to determine the fraction of the neutron star core that is superfluid as a function of time; this allows us to track the normal and superfluid components of the moment of inertia as the star ages (see Figure 3 in Supplementary Information).

We consider a simple phenomenological model for rotational evolution of the normal and superfluid components of the star:

$$\frac{d}{dt}(I\Omega) = -\beta\Omega^3 - N_{\text{pin}} - N_{\text{mf}} \quad (1)$$

$$\frac{d}{dt}(I_{\text{sf}}\Omega_{\text{sf}}) = N_{\text{pin}} + N_{\text{mf}}, \quad (2)$$

where  $I$  and  $I_{\text{sf}}$  are the moments of inertia of the normal and superfluid components, respectively, and  $N_{\text{pin}}$  and  $N_{\text{mf}}$  are torques associated with vortex pinning<sup>11</sup> and dissipative mutual friction,<sup>12</sup> respectively. Note that it is the rotation of the normal component  $\Omega$  that is observed in pulsars. There are three simple limits that we can consider. The first is that friction acts on a much shorter timescale than the spin-down timescale<sup>12</sup>; this is the conventional view of rotational evolution, which leads to  $\Omega_{\text{sf}}$  closely tracking  $\Omega$  and a braking index  $n = 3$ , at odds with all measured values.<sup>3</sup> The second limit is when there is no pinning or friction; we find that this leads to  $n > 3$ . The final case, which we consider in detail here, is when pinning causes  $\dot{\Omega}_{\text{sf}} \approx 0$  ( $\dot{x}$  is the first time derivative of

parameter  $x$ ). The evolution equations can then be combined to give

$$\frac{d\Omega}{dt} = (\Omega_{\text{sf}} - \Omega) \frac{1}{I} \frac{dI}{dt} - \beta \frac{\Omega^3}{I}. \quad (3)$$

The spin lag,  $\Omega_{\text{sf}} - \Omega$ , is the difference in rotational velocity between the superfluid and normal components. Some examples of decoupled spin evolution are shown in Figure 1.

Conventional pulsar spin evolution only accounts for the second term on the right hand side of eq. (3), with constant  $B$  and  $I$ . In this case, pulsars born at a particular spin period ( $P = 2\pi/\Omega$ ) evolve by moving along lines of constant<sup>13,14</sup>  $B$ , and the characteristic age  $\tau_c (\equiv P/2\dot{P})$  is an estimate of the true age of the pulsar. However, this again suggests that the conventional picture is incomplete: in cases where an independent age can be estimated (e.g., from studying the expansion of an associated supernova remnant), the result is often quite different from the characteristic age; this can be seen in Table 1. When superfluid decoupling is taken into account, spin evolution is similar to the conventional course, except now the moment of inertia decreases over time. If the spin lag remains small (e.g., as a result of an angular momentum sink acting on the superfluid), only a small deviation (from evolution along a constant  $B$  track) is seen at intermediate and late times (after  $\sim 1000 - 2000$  yr). Note that we are considering intermediate times ( $\sim 10^3 - 10^5$  yr) in the life of a neutron star, in between the short timescale for glitch recurrence<sup>15</sup> ( $\sim 1$  yr) and the long timescales for magnetic field diffusion<sup>13,14</sup> and cooling<sup>16–18</sup> ( $\sim 10^5 - 10^6$  yr). On the other hand, if the spin lag is allowed to become large (e.g., due to strong vortex pinning), then we see that a decreasing  $I$  can mimic a strongly increasing magnetic field. A further departure from the conventional picture is that the characteristic age is not an accurate indication of the true age of a pulsar at early times.

Not only are the spin period  $P$  and first time derivative of the period  $\dot{P}$  observable quantities, in some cases the second time derivative  $\ddot{P}$  can be measured ( $\ddot{x}$  is the second time derivative of parameter  $x$ ). This provides another test for our model. Table 1 gives data on eight systems where the braking index  $n$ , which is proportional to  $\ddot{P}$ , has been measured, while our model predicts the braking index to be [see eq. (3)]

$$n \equiv \frac{\Omega \ddot{\Omega}}{\dot{\Omega}^2} = 3 - \frac{2\dot{I}}{I} \frac{\Omega}{\dot{\Omega}} - \left( \frac{3\dot{I}}{I} \frac{\Omega}{\dot{\Omega}} - \frac{\ddot{I}}{I} \frac{\Omega^2}{\dot{\Omega}^2} \right) \left( \frac{\Omega_{\text{sf}}}{\Omega} - 1 \right). \quad (4)$$

When  $\Omega_{\text{sf}} - \Omega \ll \Omega$ , the last term is irrelevant, and the braking index is simply given by  $n = 3 - 4\tau_c |\dot{I}/I|$ .

Since  $\tau_c$  and  $n$  are observable quantities (related simply to  $P$ ,  $\dot{P}$ , and  $\ddot{P}$ ) for a given pulsar, we can compare our predictions to the pulsars in Table 1; this is shown in Figure 2. For the Crab pulsar (the only one with a known age), we infer a mass of  $\approx 1.8 M_{\text{Sun}}$  (for the particular

equation of state and superfluid properties we consider; see Supplementary Information). Furthermore, we can use the mass determination to estimate the initial period and magnetic field of the pulsar, and we find an initial period  $\sim 0.02$  s and  $B \sim 4 \times 10^{12}$  G.

The fact that our simple model is able to explain the observed pulsar properties demonstrates the merits of the notion of decoupled spin-evolution due to the onset of core superfluidity. However, key questions remain to be understood. The main assumption in our model is that core superfluid neutrons are allowed to decouple and pin. Core pinning is thought to be the result of the interaction between superfluid vortices and fluxtubes in the proton superconductor.<sup>11</sup> Whether this mechanism can be strong enough to act in the way assumed in our analysis is not clear at this time. Theoretical work is also required to determine whether the spin-lag  $\Omega_{\text{sf}} - \Omega$  can be kept small during the evolution by an (at this time) unspecified angular momentum “sink”. From an observational point-of-view, the model is promising, in particular since it can be used to infer the mass of individual pulsars. In the future, discovery and long-term monitoring of a large number of systems by radio telescopes such as LOFAR and SKA will allow accurate timing of many young pulsars. Taking these pulsars as an ensemble, we can constrain the nuclear equation of state and superfluid properties since these determine the evolution of the moment of inertia. Finally, radio timing measurements may be able to constrain neutron star thermal evolution, independent of measurements at X-ray energies.

---

Received 27 November 2018; accepted —.

1. Pacini, F. Rotating neutron stars, pulsars and supernova remnants. *Nature* **219**, 145–146 (1968).
2. Gunn, J. E. & Ostriker, J. P. Magnetic dipole radiation from pulsars. *Nature* **221**, 454–456 (1969).
3. Espinoza, C. M., Lyne, A. G., Kramer, M., Manchester, R. N., & Kaspi, V. M. The braking index of PSR J1734–3333 and the magnetar population. *Astrophys. J.* **741**, L13–1–6 (2011).
4. Lyne, A. G., Pritchard, R. S., & Graham-Smith, F. 23 years of Crab pulsar rotational history. *Mon. Not. R. Astron. Soc.* **265**, 1003–1012 (1993).
5. Migdal, A. B. Superfluidity and the moments of inertia of nuclei. *Sov. Phys. JETP* **10**, 176–185 (1960).
6. Baym, G., Pethick, C., & Pines, D. Superfluidity in neutron stars. *Nature* **224**, 673–674 (1969).
7. Heinke, C. O. & Ho, W. C. G. Direct observation of the cooling of the Cassiopeia A neutron star. *Astrophys. J.* **719**, L167–L171 (2010).
8. Shternin, P. S., Yakovlev, D. G., Heinke, C. O., Ho, W. C. G. & Patnaude, D. J. Cooling neutron star in the Cassiopeia A supernova remnant: Evidence for superfluidity in the core. *Mon. Not. R. Astron. Soc.* **412**, L108–L112 (2011).

Pulsar Name	Supernova remnant	Period (s)	Period derivative ( $\text{s s}^{-1}$ )	Characteristic age $\tau_c$ (yr)	Braking index $n$	Age (yr)
B0531+21	Crab	0.0331	$4.23 \times 10^{-13}$	1240	2.51(1) [4]	958
J0537-6910	N157B	0.0161	$5.18 \times 10^{-14}$	4930	-1.5(1) [20]	$2000^{+3000}_{-1000}$ [21]
B0540-69	0540-69.3	0.0505	$4.79 \times 10^{-13}$	1670	2.140(9) [22]	$1000^{+660}_{-240}$ [23]
B0833-45	Vela	0.0893	$1.25 \times 10^{-13}$	11300	1.4(2) [24]	$11000^{+5000}_{-5600}$ [25]
J1119-6127	G292.2-0.5	0.408	$4.02 \times 10^{-12}$	1610	2.684(2) [26]	$7100^{+500}_{-2900}$ [27]
B1509-58	G320.4-1.2	0.151	$1.54 \times 10^{-12}$	1550	2.839(3) [22]	< 21000 [28]
J1846-0258	Kesteven 75	0.325	$7.08 \times 10^{-12}$	729	2.65(1) [22]	$1000^{+3300}_{-100}$ [29]
J1734-3333	G354.8-0.8	1.17	$2.28 \times 10^{-12}$	8120	0.9(2) [3]	> 1300

**Table 1. Pulsars with observed braking index.** Periods and period derivatives are taken from ref. 19. Numbers in parentheses show braking index uncertainty in the last digit. For J1734-3333, we give a lower limit of the age, which we estimate by (1) considering the supernova remnant size (21 parsecs; ref. 30) and remnant expansion velocity  $v_{\text{SNR}}$ , in order to obtain an age  $\sim 2000$  yr ( $10^4$  km  $\text{s}^{-1}/v_{\text{SNR}}$ ) and (2) considering the pulsar’s distance away from the centre of the supernova remnant (46 parsecs; ref. 30) and pulsar space velocity  $v_{\text{pulsar}}$ , in order to obtain an age  $\sim 23000$  yr ( $2000$  km  $\text{s}^{-1}/v_{\text{pulsar}}$ ).

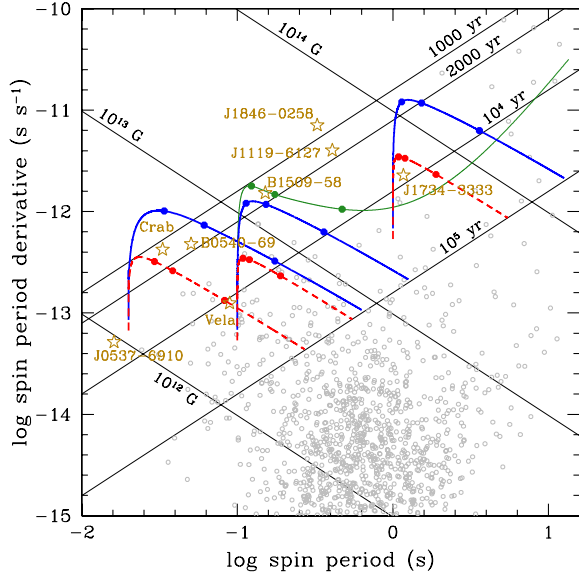


**Figure 1. Pulsar spin period versus spin period derivative.** Open circles are observed values taken from the ATNF Pulsar Catalogue.<sup>19</sup> Stars denote pulsars with a measured braking index (see Table 1). Thin diagonal lines denote characteristic age ( $= P/2\dot{P}$ ) and inferred magnetic field [ $= 3.2 \times 10^{19} \text{ G} (P\dot{P})^{1/2}$ ]. Curves are spin evolution tracks for pulsars with mass  $1.8 M_{\text{Sun}}$  (red, dashed) and  $1.4 M_{\text{Sun}}$  (blue, solid), where the spin lag is maintained at  $\Omega_{\text{sf}}/\Omega - 1 \leq 10^{-6}$  (by an additional angular momentum sink); filled circles denote the evolution at ages 1000, 2000, and  $10^4$  yr. Also shown (green, thin solid) is the evolution of a pulsar where the spin lag is allowed to grow. From left to right, the initial spin period and magnetic field ( $P, B$ ) are taken to be (0.02 s,  $5 \times 10^{12}$  G), (0.1 s,  $10^{13}$  G), and (1 s,  $10^{14}$  G).

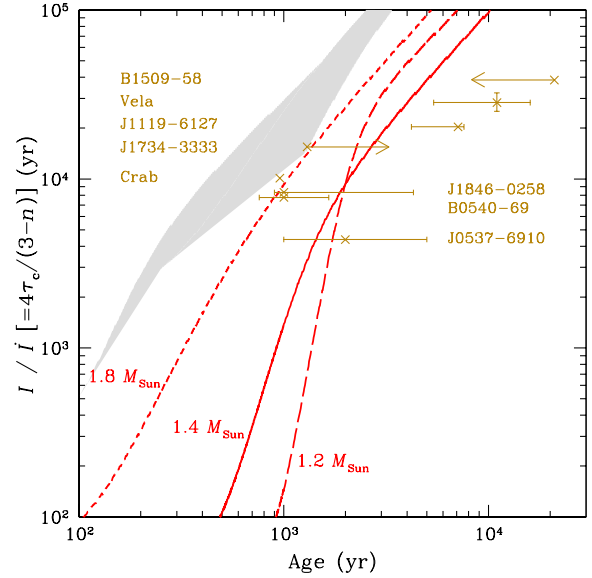


**Figure 2. Constraining neutron star properties.** Crosses denote pulsars with a measured braking index and an estimate or limit on their true age (see Table 1). Curves show the evolution of the effective moment of inertia for pulsars with mass  $1.8 M_{\text{Sun}}$  (short-dashed),  $1.4 M_{\text{Sun}}$  (solid), and  $1.2 M_{\text{Sun}}$  (long-dashed), assuming a particular stellar and superfluid model,<sup>9</sup> while the shaded region represents an alternative model<sup>8</sup>; both sets of superfluid parameters fit the rapid cooling seen in the Cassiopeia A neutron star (see Supplementary Information). These moment of inertia evolution curves are analogous to the thermal cooling curves<sup>16-18</sup> used to determine properties of neutron stars.

9. Page, D., Prakash, M., Lattimer, J. M., & Steiner, A. W. Rapid cooling of the neutron star in Cassiopeia A triggered by neutron superfluidity in dense matter. *Phys. Rev. Lett.* **106**, 081101-1-4 (2011).
10. Ho, W. C. G., Glampedakis, K., & Andersson, N. Magneters: super(ficially) hot and super(fluid) cool. *Mon. Not. R. Astron. Soc.* **422**, 2632-2641 (2012).
11. Link, B. Constraining hadronic superfluidity with neutron star precession. *Phys. Rev. Lett.* **91**, 101101-1-4 (2003).
12. Alpar, M. A., Langer, S. A., & Sauls, J. A. Rapid post-glitch spin-up of the superfluid core in pulsars. *Astrophys. J.* **282**, 533-541 (1984).
13. Goldreich, P. & Reisenegger, A. Magnetic field decay in isolated neutron stars. *Astrophys. J.* **395**, 250-258 (1992).
14. Glampedakis, K., Jones, D. I., & Samuelsson, L. Ambipolar diffusion in superfluid neutron stars. *Mon. Not. R. Astron. Soc.* **413**, 2021-2030 (2012).
15. Espinoza, C. M., Lyne, A. G., Stappers, B. W., & Kramer, M. A study of 315 glitches in the rotation of 102 pulsars. *Mon. Not. R. Astron. Soc.* **414**, 1679-1704 (2011).
16. Tsuruta, S. Thermal properties and detectability of neutron stars. II. Thermal evolution of rotation-powered neutron stars. *Phys. Rep.* **292**, 1-130 (1998).
17. Yakovlev, D. G. & Pethick, C. J. Neutron star cooling. *Annu. Rev. Astron. Astrophys.* **42**, 169-210 (2004).
18. Page, D., Geppert, U., & Weber, F. The cooling of compact stars. *Nucl. Phys. A* **777**, 497-530 (2006).
19. Manchester, R. N., Hobbs, G. B., Teoh, A., & Hobbs, M. The Australia Telescope National Facility Pulsar Catalogue. *Astron. J.* **129**, 1993-2006 (2005).
20. Middleditch, J., Marshall, F. E., Wang, Q. D., Gotthelf, E. V. & Zhang, W. Predicting the starquakes in PSR J0537-6910. *Astrophys. J.* **652**, 1531-1546 (2006).
21. Chen, Y., Wang, Q. D., Gotthelf, E. V., Jiang, B., Chu, Y.-H., & Gruendl, R. Chandra ACIS spectroscopy of N157B: a young composite supernova remnant in a superbubble. *Astrophys. J.* **651**, 237-249 (2006).
22. Livingstone, M. A., Kaspi, V. M., Gavriil, F. P., Manchester, R. N., Gotthelf, E. V. G., & Kuiper, L. New phase-coherent measurements of pulsar braking indices. *Astrophys. Space Sci.* **308**, 317-323 (2007).
23. Park, S., Hughes, J. P., Slane, P. O., Mori, K., & Burrows, D. N. A deep Chandra observation of the oxygen-rich supernova remnant 0540-69.3 in the Large Magellanic Cloud. *Astrophys. J.* **710**, 948-957 (2010).
24. Lyne, A. G., Pritchard, R. S., Graham-Smith, F., & Camilo, F. Very low braking index for the Vela pulsar. *Nature* **381**, 497-498 (1996).
25. Page, D., Lattimer, J. M., Prakash, M., & Steiner, A. W. Neutrino emission from Cooper pairs and minimal cooling of neutron stars. *Astrophys. J.* **707**, 1131-1140 (2009).
26. Weltevrede, P., Johnston, S., & Espinoza, C. M. The glitch-induced identity changes of PSR J1119-6127. *Mon. Not. R. Astron. Soc.* **411**, 1917-1934 (2011).
27. Kumar, H. S., Safi-Harb, S., & Gonzalez, M. E. Chandra and XMM-Newton studies of the supernova remnant G292.2-0.5 associated with the pulsar J1119-6127. *Astrophys. J.* **754**, 96-1-14 (2012).
28. Gaensler, B. M., Brazier, K. T. S., Manchester, R. N., Johnston, S., & Green, A. J. SNR G320.4-01.2 and PSR B1509-58: new radio observations of a complex interacting system. *Mon. Not. R. Astron. Soc.* **305**, 724-736 (1999).
29. Blanton, E. L. & Helfand, D. J. ASCA observations of the composite supernova remnant G29.7-0.3. *Astrophys. J.* **470**, 961-966 (1996).
30. Manchester, R. N. et al. in *Neutron Stars in Supernova Remnants* (eds Slane, P. O. & Gaensler, B. M.) 31 (ASP Conf. Ser. 271, Astronomical Society of the Pacific, 2002).
31. Potekhin, A. Y. & Chabrier, G. Thermodynamic functions of dense plasmas: Analytic approximations for astrophysical applications. *Contrib. Plasma Phys.* **50**, 82-87 (2010).
32. Lattimer, J. M., van Riper, K. A., Prakash, M., & Prakash, M. Rapid cooling and the structure of neutron stars. *Astrophys. J.* **425**, 802-813 (1994).
33. Gnedin, O. Y., Yakovlev, D. G., & Potekhin, A. Y. Thermal relaxation in young neutron stars. *Mon. Not. R. Astron. Soc.* **324**, 725-736 (2001).
34. Yakovlev, D. G., Ho, W. C. G., Shternin, P. S., Heinke, C. O., & Potekhin, A. Y. Cooling rates of neutron stars and the young neutron star in the Cassiopeia A supernova remnant. *Mon. Not. R. Astron. Soc.* **411**, 1977-1988 (2011).
35. Ravenhall, D. G. & Pethick, C. J. Neutron star moments of inertia. *Astrophys. J.* **424**, 846-851 (1994).

---

**Supplementary Information** is linked to the online version of the paper at [www.nature.com/nature](http://www.nature.com/nature).

**Acknowledgements.** W.C.G.H. thanks D. Yakovlev for providing equation of state tables. W.C.G.H. appreciates the use of the computer facilities at the Kavli Institute for Particle Astrophysics and Cosmology. W.C.G.H. and N.A. acknowledge support from the Science and Technology Facilities Council (STFC) in the United Kingdom.

**Author Contributions** W.C.G.H. contributed to developing the model, performed the calculations, and wrote the manuscript. N.A. contributed to developing the model and writing the manuscript.

**Author Information** Reprints and permissions information is available at [www.nature.com/reprints](http://www.nature.com/reprints). The authors declare no competing financial interests. Correspondence and requests for materials should be addressed to W.C.G.H. ([wynnho@slac.stanford.edu](mailto:wynnho@slac.stanford.edu)) or N.A. ([n.a.andersson@soton.ac.uk](mailto:n.a.andersson@soton.ac.uk)).

## Supplementary Information

### Neutron star cooling and moment of inertia evolution

Neutron stars begin their lives very hot (with temperatures  $T > 10^{11}$  K) but cool rapidly through the emission of neutrinos. Neutrino emission processes depend on uncertain physics at the supra-nuclear densities ( $\rho > 2.8 \times 10^{14}$  g cm $^{-3}$ ) of the neutron star core.<sup>16–18</sup> The recent observation of rapid cooling<sup>7,8</sup> of the neutron star in the Cassiopeia A supernova remnant provides the first constraints on the (density-dependent) critical temperatures for the onset of superfluidity of core protons  $T_{\text{cp}}$  (in the singlet state) and neutrons  $T_{\text{cnt}}$  (in the triplet state), i.e.,  $T_{\text{cp}} \sim (2-3) \times 10^9$  K and a maximum  $T_{\text{cnt}} \approx 5 \times 10^8$  K for a superfluid neutron model at relatively shallow densities<sup>9</sup> or a maximum  $T_{\text{cnt}} \approx (7-9) \times 10^8$  K for a superfluid neutron model at deep densities.<sup>8</sup>

We calculate the thermal evolution of neutron stars by solving the relativistic equations of energy balance and heat flux. We use a stellar model based on the APR equation of state and consider either the shallow or deep model for triplet neutron pairing in the core.<sup>10</sup> Note that we improve upon the calculations of ref. 10 by using more accurate ion and electron heat capacities.<sup>31</sup> Due to high thermal conductivity, neutron stars after  $\sim 10 - 100$  yr are essentially isothermal<sup>32–34</sup>; the exact time is unimportant for our work since the youngest neutron star we consider has an age  $\approx 1000$  yr (see Table 1). The evolution of the (gravitationally redshifted) surface temperature for models with the shallow neutron superfluid and an unmagnetized iron envelope is shown in Figure 3. Enhanced neutrino emission due to Cooper pairing of neutrons begins to occur at the onset of superfluidity in the core. At an age of a few hundred to one thousand years, large portions of the (predominantly neutron) stellar core become superfluid, and rapid cooling occurs.

We calculate the moment of inertia of the normal and superfluid components by<sup>35</sup>

$$I = \frac{8\pi}{3} \int_0^R (\rho + P/c^2) \Lambda r^4 dr, \quad (5)$$

where  $P$  is the local pressure,  $\Lambda = (1 - 2Gm/c^2r)^{-1}$ , and  $m$  is the mass enclosed within  $r$ . Note that we neglect for simplicity a term that approximately accounts for relativistic frame-dragging,<sup>35</sup> which would only change  $I$  by  $< 10\%$ . Figure 3 shows the evolution of the normal component of  $I$ .

In order to facilitate numerical calculations of  $\dot{I}(t)$  and  $\ddot{I}(t)$ , we fit  $I(t)$  with the following function

$$\log I = a_3 \tanh[a_2(\log t - a_1)] + (\log t - b_1)^{b_2} + c_1, \quad (6)$$

where the fit parameters  $a_1, a_2, a_3, b_1, b_2, c_1$  are given in Table 2. A comparison of the approximate fit to the exact

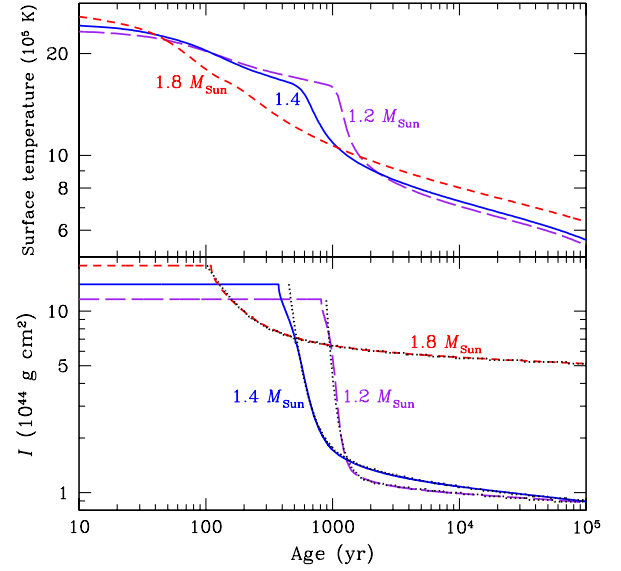


**Figure 3. Thermal and moment of inertia evolution of neutron stars.** Curves show the evolution of the surface temperature (top) and moment of inertia (bottom) for neutron stars with mass  $1.8 M_{\text{Sun}}$  (red, short-dashed),  $1.4 M_{\text{Sun}}$  (blue, solid), and  $1.2 M_{\text{Sun}}$  (purple, long-dashed). Dotted curves show analytic fits using eq. (6).

Neutron star mass	$a_1$	$a_2$	$a_3$	$b_1$	$b_2$	$c_1$
$1.2 M_{\text{Sun}}$	2.90	7.4	-1.5	0.10	-1.0	45.24
$1.4 M_{\text{Sun}}$	2.59	4.6	-1.2	0.95	-1.2	44.97
$1.8 M_{\text{Sun}}$	1.98	2.6	-0.31	0	-1.6	44.945

**Table 2. Fit parameters for moment of inertia evolution.**

result is shown in Figure 3. Note that the largest deviations occur briefly at (early) times that are not of current relevance.